SUMO User Conference 2026
Conference Paper
DOI: -

Published: -

VRU-Aware GLOSA: Integrating VRUs into Green Light Optimized Speed Advisory for Right-Turn Conflicts at Signalized Intersections

Pushkar Mahajan[1], Anna-Lena Schlamp [1], and Stefanie Schmidtner[1]

[1]Technische Hochschule Ingolstadt, Germany

*Correspondence: Pushkar Mahajan, Pushkar.Mahajan@thi.de

Abstract: Urban signalized intersections remain safety-critical despite phase-based control, particularly in scenarios where right-turning vehicles and straight-going Vulnerable Road Users (VRUs) approach from the same direction and may enter a shared conflict area with overlapping arrival times. This risk is amplified by the increasing prevalence of electric bicycles, whose higher speeds and accelerations reduce the available reaction time. Green Light Optimized Speed Advisory (GLOSA) can improve efficiency by coordinating vehicle approach speeds with Signal Phase and Timing (SPaT), but conventional implementations are largely vehicle-centric and do not explicitly manage VRU conflicts. This paper presents a VRU-aware GLOSA that augments classical SPaT-based speed advice with a conflict-aware safety overlay. We evaluate three strategies in SUMO: baseline (no advisory), classical queue-compensated GLOSA, and VRU-aware GLOSA. The simulation is based on a digital twin of a real-world signalized intersection in Ingolstadt, Germany. Results demonstrate that VRU-aware GLOSA successfully improves safety by reducing conflicts and increasing temporal gaps, while also enhancing traffic flow through fewer vehicle stops across diverse bicycle types and riding styles.

Keywords: Vulnerable Road Users (VRUs), Green Light Optimized Speed Advisory (GLOSA), Right-Turn Conflicts, Safety, Bicycle Riding Styles

1 Introduction

Vulnerable Road Users (VRUs), such as pedestrians and cyclists, are the most at-risk participants in urban traffic, accounting for more than 50% of global road traffic fatalities [1]. At signalized intersections, conflicts between right-turning vehicles and straight-going VRUs during permissive green phases remain a critical safety concern, driven by limited driver visibility due to vehicle blind spots and the inherently variable behavior of VRUs [2]. The growing prevalence of electric bicycles with higher operating speeds further amplify these risks by reducing driver reaction times and increasing the likelihood of misjudgment [3], [4]. Given the European Vision Zero [5], which aims to eliminate traffic fatalities by 2050, effective measures to reduce VRU-related risks are essential. Common approaches, such as dedicated signal phases and sensor-based driver warning systems, can reduce conflicts but often compromise traffic efficiency and intersection throughput due to abrupt braking or delays. Proactive vehicle control is therefore essential to jointly enhance VRU safety and traffic efficiency. It has also been shown to build trust and improve perceived safety from a VRU perspective [6], [7]. To address this, we present a VRU-aware Green Light Optimized Speed Advisory (GLOSA) system that incorporates VRU interactions into vehicle speed guidance.

1.1 GLOSA and Eco-Driving at Signalized Intersections

GLOSA is a well-established approach for proactively optimizing vehicle speed on signalized road networks to improve traffic efficiency. It estimates a vehicle's expected arrival time at the next traffic light based on its current position and dynamic state, and predicts the upcoming signal phases using Signal Phase and Timing (SPaT) information. Based on this, an optimal speed within legal limits is computed, deciding whether to maintain, accelerate, or decelerate to efficiently pass the intersection during a green phase [8]–[10]. Existing GLOSA implementations predominantly rely on physics-based calculation models, whereas advanced eco-driving approaches formulate speed optimization as an analytical [11], [12] or AI-based problem [13]–[15]. Several studies further extend classical GLOSA by incorporating queue awareness, as preceding vehicles and waiting queues have been shown to negatively affect its performance [13], [16]. GLOSA can be deployed in mixed traffic environments, either by providing advisory speeds to human-driven Connected Vehicles (CVs) or by directly controlling Connected and Automated Vehicles (CAVs). Prior studies consistently report improvements in travel time, waiting time, fuel consumption, and emissions, even at moderate penetration rates, with observed positive impacts on non-equipped vehicles [8].

At urban signalized intersections with right-turn vehicle–VRU conflicts, smoother vehicle behavior does not necessarily prevent temporal overlap, as both road users may still enter the shared conflict area within insufficiently separated time windows. Consequently, safety-related indicators may remain unchanged even when upstream traffic flow becomes smoother. This limitation motivates extension of GLOSA that explicitly account for VRU interactions to enhance safety. However, existing GLOSA research predominantly focuses on efficiency metrics while safety impacts are less frequently evaluated and rarely analyzed in the context of VRUs [8]–[10].

1.2 Vulnerable Road Users in GLOSA

Current GLOSA and eco-driving designs do not explicitly account for VRUs. From an efficiency perspective, this leaves unused potential since right-turning vehicles – after crossing the stop line – still need to brake and wait for passing VRUs. From a safety perspective, critical right-turn vehicle–VRU conflicts remain largely unaddressed. Integrating VRU-awareness into GLOSA offers the potential to simultaneously improve vehicle efficiency and VRU safety. Sensor-equipped testbeds, such as the High Definition Testbed (HDT) in Ingolstadt [17], as well as CVs acting as Floating Car Observers (FCOs) [18] and continuously broadcasting their local perception via Vehicle-to-Everything (V2X) communication, can provide the necessary VRU state information in real-world settings. However, the extent to which VRU-aware GLOSA can enhance safety and efficiency under realistic traffic conditions remains unclear. This motivates a controlled evaluation in a digital twin of a real-world intersection, establishing baseline expectations for subsequent studies on real-world testbeds that consider perception, communication, and prediction uncertainties and latency.

1.3 Bicycle Types and Riding Styles

Cyclists are highly vulnerable in right-turn conflicts with vehicles [2]. The risk is particularly elevated for higher-speed electric bicycle types such as e-bikes and S-pedelecs, with e-bikes typically limited to electric assistance up to 25 km/h and S-pedelecs up to 45 km/h. Given their diverse dynamic characteristics, it is essential to account for variations in bicycle type and riding styles when analyzing safety and efficiency at signalized intersections. However, research on realistic bicycle behavior models remains limited, largely due to scarce high-resolution data on speed profiles, acceleration, and braking characteristics. Existing evidence primarily stems from (i) naturalistic cycling studies and (ii) controlled experiments. Naturalistic studies consistently show that operating speeds depend on both bicycle type and rider attributes: S-pedelecs exhibit the highest speeds, and age is a strong determinant of cycling speed [19], [20]. They further indicate that switching from a conventional bicycle to an e-bike increases travel speeds and alters braking behavior, implying modified interaction dynamics at shared conflict points [21]. Experimental studies complement these findings by quantifying differences in riding performance and longitudinal control, revealing systematic variations for older riders as well as differences in acceleration and braking characteristics relevant for trajectory prediction and conflict assessment [22], [23]. Importantly, several studies highlight a confounding effect between bicycle type and rider age group: older riders are overrepresented among e-bike users and tend to ride more slowly, potentially masking the higher assisted capabilities of these bicycles when analyses do not stratify by age [19], [20]. Overall, the limited availability of differentiated behavior models and the confounding between bicycle type and rider characteristics indicate a clear need for systematic research that disentangles their effects on safety and efficiency at signalized intersections.

1.4 Contributions

Building on the research gaps outlined above, this paper makes the following contributions:

- We develop a VRU-aware GLOSA that augments classical GLOSA with a VRU-aware overlay, combining SPaT information with predicted arrival times to anticipate right-turn conflicts and optimize speed accordingly.
- We evaluate the proposed VRU-aware GLOSA in comparison to classical GLOSA without VRU awareness and a no-GLOSA baseline within a digital twin of our testbed intersection, modeling realistic traffic conditions. The evaluation jointly examines safety and efficiency metrics, with a specific focus on right-turn conflicts between vehicles and cyclists.
- In a second approach, we model realistic bicycle types and riding styles within the simulation and systematically evaluate the VRU-aware GLOSA to assess how diverse behavior characteristics influence safety and efficiency outcomes.

To support further research, we make the source code and VRU-integrated digital twin developed in this work available at: https://github.com/urbanAIthi/VRU_Aware_GLOSA.git.

2 VRU-aware Green Light Optimized Speed Advisory

In this work, we enhance classical GLOSA by integrating explicit awareness of right-turn conflicts with straight-going VRUs into signal-based speed advisory. The proposed VRU-aware overlay comprises two core components: conflict prediction and speed optimization. Operating in parallel with classical GLOSA, the overlay proactively delays right-turning vehicles upstream of the stop line by overriding the nominal speed advisory when conflicts are predicted, thereby ensuring temporal separation.

Conflict Prediction: We define a VRU-aware activation region covering the last 50 meters upstream of the stop line, within which all vehicles and VRUs are evaluated for potential conflicts. The algorithm takes as input the upcoming signal phases as well as the current kinematic states of vehicles and VRUs. For each right-turning vehicle, the estimated time-to-arrival (ETA) at the junction, η_{veh}, is computed from its remaining distance d_{veh}, speed v_{GLOSA}, and acceleration – defined by classical GLOSA – using a queue-aware kinematic model [13]. For each candidate VRU, we predict whether it will traverse the intersection by jointly considering (i) the SPaT forecast for the corresponding VRU signal group and (ii) the VRU ETA, η_{vru}. A conflict is detected if the vehicle and VRU ETAs overlap within a symmetric time window Δt (Eq. (1)). We set Δt = 2 s as a conservative minimum temporal separation threshold. This is motivated by general road-safety guidance underlying the widely used two-second rule, which supports sufficient reaction time and conflict avoidance [24]. Multiple VRUs may conflict with a single vehicle, resulting in a set of conflicting VRUs $\mathcal{C}$.

$$|\eta_{\text{veh}} - \eta_{\text{vru}}| \leq \Delta t, \qquad \Delta t = 2 \text{ s} \tag{1}$$

Speed Optimization: Vehicle motion is initially governed by classical GLOSA, operating in parallel. We employ the queue-aware GLOSA proposed in [13] as the nominal advisory layer. This approach combines SPaT information with queue effects from preceding vehicles to derive a feasible speed advisory, since queue interactions can adversely affect GLOSA performance under high traffic demand. To account for straight-going VRUs, the nominal speed advisory is overridden by a conservative yielding strategy whenever a potential right-turn conflict is predicted (see Algorithm 1). This strategy deliberately delays vehicles upstream of the stop line to enforce sufficient temporal separation. The yielding speed is computed using a classical kinematic model to ensure that the vehicle reaches the intersection at least Δt after the last conflicting VRU, defined as

$$v_{\text{yield}} = \frac{d_{\text{veh}}}{\eta_{\text{vru,last}} + \Delta t} \tag{2}$$

where d_{veh} denotes the vehicle's remaining distance to the conflict point. Here, $\eta_{\text{vru,last}}$ denotes the latest predicted arrival time among all VRUs in the conflict set $\mathcal{C}(i)$, i.e., $\eta_{\text{vru,last}} = \max_{j \in \mathcal{C}(i)} \eta_{\text{vru},j}$. Thus, $\eta_{\text{vru,last}} + \Delta t$ defines the target ETA such that the vehicle reaches the intersection at least Δt after the last conflicting VRU, ensuring conflict avoidance with all VRUs predicted to traverse the intersection.

Algorithm 1 VRU-aware GLOSA overlay

Inputs: GLOSA advisory v_{GLOSA}, vehicle/VRU states, SPaT forecast
Parameters: Temporal headway Δt
Compute η_{veh} for vehicle i.
For each candidate VRU in range, compute η_{vru} using the SPaT forecast.
Predict set of conflicting VRUs $\mathcal{C}$ for vehicle i based on overlapping vehicle and VRU ETAs.
if $\mathcal{C}(i) \neq \varnothing$ **then**
    Compute v_{yield} based on remaining distance d_{veh} and target ETA $\eta_{\text{vru,last}} + \Delta t$.
else
    Maintain nominal speed advisory v_{GLOSA}.
end if

3 Evaluation Setup

For evaluation, we use the vehicle-centric traffic system developed in [25], which represents a digital twin of the city of Ingolstadt, featuring a realistic road network and traffic demand modeled in SUMO [26]. It thereby serves as a realistic experimental basis for evaluating the proposed control strategy rather than for recalibrating the full scenario. The GLOSA algorithms are tested at a single signalized intersection, specifically the HDT intersection (see Fig. 1), selected for its equipped infrastructure-based sensing, high VRU volumes, and frequent right-turn conflicts, enabling future validation in real-world settings. As an initial step to evaluate the proposed strategy in a controlled setting while minimizing scenario complexity, our analysis focuses on a single approach (south to north), with two lanes per direction, no overtaking, and maneuver-specific lane use. Vehicle demand follows [25], while VRU flows are synthesized using the same temporal profile and scaled to 25% of vehicle traffic, consistent with [27]. Traffic signals operate on fixed-time control with real-world phase durations [25], allowing vehicles to access current and future phase information. VRU signal phases are shorter than vehicle phases and include a one-second head start, reflecting common VRU-prioritization practice.

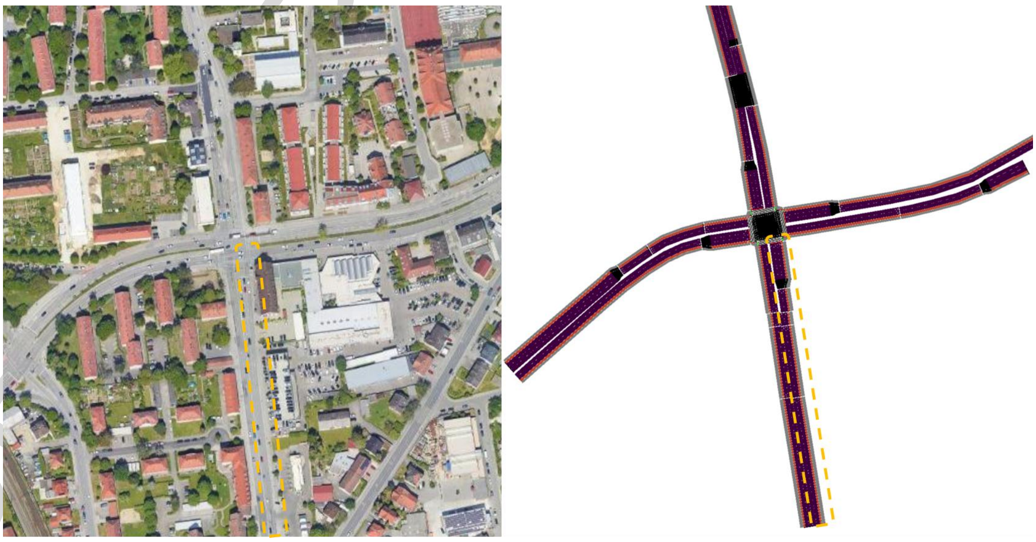

Figure 1. Real-world (left) and SUMO-simulated (right) layouts of the HDT signalized intersection, with the approach for improving vehicle–-VRU interactions highlighted.

Two simulation studies are conducted, considering interactions between right-turning vehicles and straight-going VRUs at the shared conflict area. VRUs are explicitly modeled as cyclists to capture their higher operating speeds, increased collision risk, and variability in bicycle types. In SUMO, cyclists are represented as slow-moving vehicles, with only speed, acceleration, and deceleration varied to reflect bicycle type and riding style, while all other parameters remain at their default values. This simplified abstraction is consistent with current microscopic VRU simulation practice, where cyclists are typically represented using adapted lane-based models [28]. Study A simulates a real-world 12-hour period to capture time-varying traffic conditions. Study B performs a systematic sensitivity analysis during peak hour with different bicycle behavior characteristics to quantify their impact on safety and efficiency improvements of VRU-aware GLOSA. The corresponding parameterization is summarized in Tables 3 and 4. Three approaches are compared under identical simulation settings: (1) a baseline without speed advisory [29]; (2) classical queue-aware GLOSA without VRU consideration [13]; and (3) the proposed VRU-aware GLOSA. All scenarios use identical SUMO default vehicle dynamics and right-of-way logic. In the GLOSA scenarios, the advisory adjusts the approach speed of equipped right-turning vehicles while SUMO's motion logic remains active. In safety-critical situations, VRU-aware GLOSA can enforce stronger but feasible deceleration. All right-turning vehicles on the studied approach are included in the evaluation and assumed to be CAVs, adapting to speed advisories issued at 10 Hz to capture short-horizon interactions and dynamic traffic conditions.

Since microscopic traffic simulation is typically collision-free under normal operation, safety is assessed using surrogate measures rather than crash counts. Accordingly, we use Time-To-Collision (TTC), which measures the predicted time until a vehicle and VRU would collide, and Post-Encroachment Time (PET), which captures the temporal gap between their traversals at the shared conflict area. TTC and PET are categorized into discrete intervals: TTC values are split into $\leq$ 1.0 s and $>$ 1.0 s, while PET values are reported as cumulative threshold shares at $\geq$ 1.5 s, $\geq$ 2.0 s, and $\geq$ 2.5 s, highlighting the proportion of interactions attaining progressively larger temporal safety margins. Vehicle efficiency is quantified using travel time, waiting time, number of stops, CO_2 emissions (based on SUMO's standardized EURO4 vehicle model), and red-wait time (time stopped while the next signal is red). All safety and efficiency metrics are computed exclusively for right-turning vehicles on the evaluated approach. Safety outcomes are reported as absolute percentage point (pp) differences, whereas efficiency metrics are expressed as relative percentage changes averaged over all right-turning vehicles.

4 Study A: Real-World Setting with Mixed Bicycle Traffic

Study A evaluates the three strategies (baseline, classical GLOSA, and VRU-aware GLOSA) over a 12-hour period (00:00–12:00) using the digital twin described in Section 3. Bicycle traffic is modeled as a 50/50 mixture of conventional bicycles and e-bikes, reflecting recent market sales shares in Germany [30]. Bicycle riding styles are parameterized using average edge speeds from the naturalistic cycling dataset presented in [20].

Safety outcomes, summarized in Table 1, indicate that VRU-aware GLOSA substantially improves temporal separation between right-turning vehicles and VRUs. For PET, the share of interactions with large temporal gaps increases substantially: VRU-aware GLOSA yields 54% of interactions with PET $\geq$ 2.5 s, compared to only 2% for the baseline and 5% for classical GLOSA, corresponding to gains of 52 and 50 percentage points. Similar improvements are observed at PET thresholds of 2.0 s and 1.5 s, indicating that a larger share of interactions attains progressively safer temporal separations. TTC analysis confirms these findings: critical conflicts with TTC $\leq$ 1 s decrease from around 72% for the baseline and 70% for classical GLOSA to 41% with VRU-aware GLOSA, corresponding to a reduction of about 30pp. In contrast, classical GLOSA offers marginal improvement over the baseline in PET and TTC, underscoring that explicit consideration of VRUs is essential for safe right-turn maneuvers.

Table 1. *Study A: Safety outcomes of right-turn vehicle–VRU interactions (PET and TTC shares) and gains relative to baseline and classical GLOSA in percentage points (pp, with negative values giving improvements).*

Parameter	Time Threshold	Baseline	GLOSA	VRU-aware GLOSA	Gain over Baseline (pp)	Gain over GLOSA (pp)
3*PET	$\geq$ 1.5 s	86.5%	86.6%	90.8%	-4.3	-4.2
	$\geq$ 2.0 s	60.6%	60.5%	77.5%	-16.9	-17.0
	$\geq$ 2.5 s	2.4%	4.7%	54.3%	-51.9	-49.6
2*TTC	$\leq$ 1.0 s	71.8%	70.3%	40.5%	+31.3	+29.8
	$>$ 1.0 s	28.2%	29.7%	59.5%	-31.3	-29.8

Efficiency improvements for right-turning vehicles are summarized in Table 2. Both classical and VRU-aware GLOSA slightly increase average travel time (by up to 2%) due to conservative driving behavior. However, VRU-aware GLOSA reduces stops by around 21% relative to classical GLOSA and 32% relative to the baseline, enhancing traffic smoothness. Waiting and red-light times increase slightly compared to classical GLOSA, reflecting safety-driven yielding, while CO_2 emissions remain largely unchanged. Overall, VRU-aware GLOSA improves traffic flow by significantly reducing idling and stop-and-go events while maintaining VRU safety, thereby effectively balancing the trade-off between efficiency and safety.

Table 2. *Study A: Right-turn vehicle efficiency and relative improvements (negative values indicate gains).*

Parameter	Baseline	GLOSA	VRU-aware GLOSA	% Change vs Baseline	% Change vs GLOSA
Avg. Travel Time (s)	60.7	61.4	61.7	+1.6%	+0.5%
Avg. Waiting Time (s)	16.5	10.3	10.9	-34.0%	+6.1%
Avg. Stops (count)	0.9	0.8	0.6	-32.2%	-21.3%
Avg. CO_2 (g)	152.7	147.4	147.3	-3.5%	-0.1%
Avg. Red-Wait Time (s)	34.7	26.3	27.1	-21.9%	+3.0%

5 Study B: Systematic Comparison across Bicycle Behavior Models

Study B conducts a systematic sensitivity analysis during peak hour (11:00–12:00) to quantify how diverse bicycle behavior characteristics affect safety and efficiency improvements of VRU-aware GLOSA. We model nine behavior models by combining three bicycle types (conventional bicycle, e-bike, S-pedelec) with three age groups ($<$40, 40–60, $>$60) representing diverse riding styles. Each scenario includes only one bicycle-type/age-group combination with the full VRU demand assigned, thereby isolating the effect of each behavior model. Desired speeds are parameterized as age-dependent edge speeds based on a naturalistic cycling dataset [20], as presented in Table 3. Longitudinal dynamics – comfort acceleration, comfort deceleration, emergency deceleration – for conventional bicycles and e-bikes are adopted from [23]. For S-pedelecs, comfort acceleration is derived from [19], emergency deceleration is conservatively set to 5.0 m/s^2, and comfort deceleration is computed using the mean comfort-to-emergency ratio reported in [23]. All acceleration and braking parameters are summarized in Table 4.

Table 3. *Desired bicycle speeds by age group (km/h).*

Age Group	Conv	E-bike	S-ped
< 40	21.04	23.65	29.14
40–60	19.82	22.69	29.00
> 60	15.21	19.05	17.61

Table 4. *Bicycle acceleration and braking parameters (m/s^2).*

Parameter	Conv	E-bike	S-ped
Comfort Acceleration	0.45	0.70	1.20
Comfort Deceleration	1.50	1.65	2.15
Emergency Deceleration	3.60	3.66	5.00

Table 5 reports PET and TTC shares across bicycle types and rider age groups for all three control strategies, showing that the safety improvements observed in Study A persist across diverse riding behavior. Across all age groups, VRU-aware GLOSA consistently increases the share of interactions with larger temporal separations, particularly for higher thresholds (PET $\geq$ 2.5 s), reflecting enhanced conflict mitigation relative to the baseline and classical GLOSA. The improvements are most pronounced for younger riders ($<$ 40) and faster bicycle types (e-bikes and S-pedelecs). Likewise, TTC distributions reveal a substantial reduction in critical encounters (TTC $\leq$ 1 s) under VRU-aware GLOSA, demonstrating that the overlay effectively reduces high-risk right-turn interactions across diverse behavior characteristics.

With respect to right-turn vehicle efficiency across bicycle types and riding styles, VRU-aware GLOSA reduces the number of stops by 15–33% compared to classical GLOSA and by 24–33% relative to the baseline (see Table 6), indicating smoother traffic flow. Average travel times increase slightly for older riders relative to classical GLOSA, while younger riders cause modest reductions compared to the baseline. Waiting and red-light times show minor variations with bicycle type and rider age, reflecting the safety-driven yielding of the overlay, while CO_2 emissions remain largely unchanged. Overall, the results indicate that VRU-aware GLOSA can preserve its safety benefits while reducing stop-and-go events even under heterogeneous bicycle behavior, though the extent of improvement depends on riding speed. While it may introduce minor increases in travel time due to prioritizing safety, these effects diminish as bicycle speeds increase.

Table 5. *Study B: PET and TTC shares (%) for right-turn vehicle–VRU interactions across bicycle types and rider age groups.*

2***Age Group**	2***Threshold**	**Baseline**			**GLOSA**			**VRU-aware GLOSA**		
		Conv	**E-bike**	**S-ped**	**Conv**	**E-bike**	**S-ped**	**Conv**	**E-bike**	**S-ped**
PET										
3*< 40	≥ 1.5 s	63.0	57.8	52.8	61.4	58.7	43.2	84.4	78.3	66.7
	≥ 2.0 s	47.8	22.2	8.3	47.7	21.7	8.1	66.7	45.7	48.7
	≥ 2.5 s	2.2	2.2	0.0	0.0	4.3	2.7	42.2	39.1	43.6
3*40–60	≥ 1.5 s	97.6	61.4	52.8	100.0	63.6	43.2	84.4	83.7	68.4
	≥ 2.0 s	47.6	25.0	8.3	45.2	25.0	8.1	57.8	48.8	47.4
	≥ 2.5 s	2.4	2.3	0.0	0.0	4.5	2.7	40.0	37.2	42.1
3*> 60	≥ 1.5 s	100.0	97.6	100.0	100.0	100.0	100.0	90.0	83.7	91.9
	≥ 2.0 s	63.2	21.4	0.0	60.5	16.3	2.6	72.5	53.5	51.4
	≥ 2.5 s	2.6	2.4	0.0	0.0	2.3	0.0	42.5	46.5	51.4
TTC										
2*< 40	≤ 1.0 s	69.6	97.8	97.2	77.3	93.5	91.9	46.7	56.5	48.7
	> 1.0 s	30.4	2.2	2.8	22.7	6.5	8.1	53.3	43.5	51.3
2*40–60	≤ 1.0 s	50.0	97.7	97.2	54.8	93.2	91.9	46.7	51.2	52.6
	> 1.0 s	50.0	2.3	2.8	45.2	6.8	8.1	53.3	48.8	47.4
2*> 60	≤ 1.0 s	50.0	78.6	73.7	57.9	72.1	71.1	45.0	41.9	40.5
	> 1.0 s	50.0	21.4	26.3	42.1	27.9	28.9	55.0	58.1	59.5

Table 6. *Study B: Efficiency gains (in %) of VRU-aware GLOSA across behavior models relative to baseline (3 vs. 1) and relative to GLOSA (3 vs. 2). Negative values indicate improvement; positive values indicate degradation.*

2***Age Group**	2***Parameter**	**Conv**		**E-bike**		**S-ped**	
		3 vs 1	**3 vs 2**	**3 vs 1**	**3 vs 2**	**3 vs 1**	**3 vs 2**
5*< 40	Avg. Travel Time (s)	+3.4	+0.9	+3.0	+0.9	+1.8	+0.3
	Avg. Waiting Time (s)	-25.1	+11.9	-28.2	+9.3	-30.0	+9.4
	Avg. Stops (count)	-31.4	-19.2	-26.5	-16.8	-30.2	-18.8
	Avg. CO_2 (g)	-1.7	-0.1	-2.0	+0.3	-2.5	+0.1
	Avg. Red-Wait Time (s)	-14.7	+3.6	-15.9	+3.6	-15.9	+4.7
5*40–60	Avg. Travel Time (s)	+4.2	+1.8	+2.9	+0.6	+1.7	+0.2
	Avg. Waiting Time (s)	-21.3	+15.7	-29.9	+7.7	-29.8	+9.7
	Avg. Stops (count)	-28.9	-18.0	-33.3	-23.4	-29.5	-18.0
	Avg. CO_2 (g)	-2.0	+1.0	-2.4	-0.2	-2.5	-0.0
	Avg. Red-Wait Time (s)	-13.6	+4.5	-14.3	+6.1	-15.4	+5.2
5*> 60	Avg. Travel Time (s)	+9.4	+7.1	+4.2	+1.9	+5.4	+3.2
	Avg. Waiting Time (s)	-6.7	+39.5	-22.8	+14.8	-20.6	+20.0
	Avg. Stops (count)	-28.2	-14.4	-32.1	-22.5	-24.5	-13.0
	Avg. CO_2 (g)	+2.1	+4.3	-1.1	+0.9	-0.4	+1.9
	Avg. Red-Wait Time (s)	-5.2	+15.0	-10.6	+6.0	-10.6	+9.1

6 Discussion and Conclusion

This paper introduced VRU-aware GLOSA, a conflict-aware extension of SPaT-based speed advisory designed to explicitly address vehicle–-VRU interactions at signalized intersections. The approach was evaluated in a realistic digital twin of an urban traffic network under mixed bicycle traffic conditions. In addition, a second study systematically examined differences across bicycle types and riding styles.

Results show that VRU-aware GLOSA, in contrast to classical GLOSA, consistently increases temporal safety margins, reflected by higher PET and TTC values, and substantially reduces critical TTC $\leq$ 1 s encounters relative to both the baseline and classical GLOSA. These safety improvements are achieved alongside smoother vehicle operation, including fewer stops and largely unchanged emissions, but with slight increases in average travel time due to safety-driven yielding. The systematic comparison across bicycle types and riding styles shows that these safety benefits persist across diverse behavior characteristics, but vary depending on bicycle dynamics and typical operating speeds. The most pronounced safety improvements are observed for higher-speed bicycle types, such as e-bikes and S-pedelecs, and for faster riding styles represented by younger age groups. For conventional bicycles and slower riding styles, interactions naturally exhibit larger temporal separations, resulting in lower baseline conflict probabilities and smaller attainable improvements. With respect to vehicle efficiency, a substantial reduction in stops is achieved across all bicycle types and riding styles, accompanied by only minor increases in delay due to safety-driven yielding. This cost depends on bicycle dynamics: slower bicycles tend to prolong the yielding phase, whereas faster bicycles clear the conflict area more quickly and align more effectively with coordinated vehicle arrivals. Overall, the findings indicate that explicitly integrating vehicle–VRU conflicts into GLOSA substantially improves safety at right-turn conflict areas, while reducing stop-and-go behavior at the cost of small travel-time penalties. Importantly, the results suggest increasing relevance and effectiveness of the approach in traffic environments with growing shares of e-bikes and S-pedelecs. The study further underscores the importance of accounting for bicycle types with different dynamics and heterogeneous riding styles when evaluating bicycle-related traffic control strategies.

This study has some limitations. The evaluation focuses on a single signalized intersection with fixed-time control, and is restricted to modeling bicycles as VRUs, while pedestrians and e-scooters are not explicitly considered. E-scooters were not modeled separately, as their legally restricted maximum speed in Germany (20 km/h) and longitudinal speed range is largely covered by the lower-speed bicycle types included in this study. Nevertheless, the proposed framework is directly applicable to heterogeneous VRU groups. A further limitation lies in the simplified representation of VRU behavior in microscopic simulation. Both bicycle and vehicle behavior are represented using standard SUMO models. In particular, cyclists are typically represented using adapted vehicle-based models rather than dedicated bicycle-specific models [28], despite recent work emphasizing the need for more realistic and better-calibrated cyclist representations, particularly at intersections [31]. Consequently, while microscopic simulation provides a suitable basis for evaluating VRU-aware GLOSA, the results remain inherently dependent on the chosen VRU abstraction level. In addition, the evaluation assumes full knowledge of traffic states, thereby neglecting errors and uncertainties in perception or communication. Moreover, all right-turning vehicles on the studied approach are assumed to be equipped CAVs to isolate the upper-bound effect of the proposed advisory.

Future work should validate VRU-aware GLOSA in real-world testbeds, assess its robustness under realistic infrastructure- or FCO-based sensing and communication conditions, and examine mixed-traffic effects. In addition, VRU-aware GLOSA can be extended to all approaches of the intersection as well as to automated intersection control settings. Furthermore, dedicated modeling of additional VRU types, such as pedestrians and e-scooters, together with improved empirical data on riding styles and the integration of realistic bicycle dynamic models, would enable more realistic simulations and enhance the evaluation of VRU-aware GLOSA and other bicycle-related traffic control functions.

Data Availability Statement

The source code used in this study is publicly available at the following GitHub repository: https://github.com/urbanAIthi/VRU_Aware_GLOSA.git.

Author Contributions

Pushkar Mahajan: Conceptualization, Methodology, Investigation, Formal analysis, Writing – original draft, Writing – review & editing.

Anna-Lena Schlamp: Conceptualization, Methodology, Writing – original draft, Writing – review & editing.

Stefanie Schmidtner: Conceptualization, Supervision, Project administration, Funding Acquisition, Writing – review & editing.

All authors reviewed and approved the final manuscript.

Competing Interests

The authors declare that they have no competing interests.

Funding

This work was partially funded by the Bavarian State Ministry of Science and the Arts (Bayerisches Staatsministerium für Wissenschaft und Kunst, StMWK) under the research project 'SiRaMiS – Sicherheit von Radfahrern im Mischverkehr mit intelligenten Verkehrsteilnehmern und intelligenter Straßeninfrastruktur'.

References

[1] World Health Organization. "Road traffic injuries." (2023), [Online]. Available: https://www.who.int/news-room/fact-sheets/detail/road-traffic-injuries.

[2] T. S. Buch and S. U. Jensen, "Incidents between straight-ahead cyclists and right-turning motor vehicles at signalised junctions.," *Accident; analysis and prevention*, vol. 105, pp. 44–51, 2017. DOI: 10.1016/j.aap.2016.07.035.

[3] Statistisches Bundesamt (Destatis). "Korrektur: Jedes sechste todesopfer im straßenverkehr 2024 war mit dem fahrrad unterwegs." Pressemitteilung Nr. N020 vom 24. April 2025. (2025), [Online]. Available: https://www.destatis.de/DE/Presse/Pressemitteilungen/2025/04/PD25_N020_461.html.

[4] Statistisches Bundesamt (Destatis). "Verletzte bei verkehrsunfällen nach art der verkehrsbeteiligung." (2025), [Online]. Available: https://www.destatis.de/DE/Themen/Gesellschaft-Umwelt/Verkehrsunfaelle/Tabellen/verletzte-fahrzeugart.html.

[5] European Commission. "Mobility and transport - road safety." (2015), [Online]. Available: https://road-safety.transport.ec.europa.eu/index_en.

[6] D. Dey, B. M. Kuhl, B. Eggen, and J. M. B. Terken, "The impact of vehicle appearance and vehicle behavior on pedestrian interaction with autonomous vehicles," *Proceedings of the 9th International Conference on Automotive User Interfaces and Interactive Vehicular Applications Adjunct*, 2017. DOI: 10.1145/3131726.3131750.

[7] F. Schneemann and I. Gohl, "Analyzing driver-pedestrian interaction at crosswalks: A contribution to autonomous driving in urban environments," *2016 IEEE Intelligent Vehicles Symposium (IV)*, pp. 38–43, 2016. DOI: 10.1109/IVS.2016.7535361.

[8] K. Katsaros, R. Kernchen, M. Dianati, and D. Rieck, "Performance study of a green light optimized speed advisory (glosa) application using an integrated cooperative its simulation platform," *International Wireless Communications and Mobile Computing Conference (IWCMC) 2011*, Jul. 2011. DOI: 10.1109/IWCMC.2011.5982524.

[9] M.-A. Lèbre, F. L. Mouël, E. Ménard, A. Garnault, B. Bradaï, and V. Picron, "Real scenario and simulations on glosa traffic light system for reduced co2 emissions, waiting time and travel time," *ArXiv*, vol. Vol. abs/1506.01965, Jun. 2015.

[10] C. Masera, M. Imprialou, L. C. S. Budd, and C. Morton, "Estimating the traffic impacts of green light optimal speed advisory systems using microsimulation," 2019.

[11] C. Sun, J. Guanetti, F. Borrelli, and S. J. Moura, "Optimal eco-driving control of connected and autonomous vehicles through signalized intersections," *IEEE Internet of Things Journal*, vol. 7, pp. 3759–3773, 2020. DOI: 10.1109/JIOT.2020.2968120.

[12] H. Xia, G. Wu, K. Boriboonsomsin, and M. J. Barth, "Development and evaluation of an enhanced eco-approach traffic signal application for connected vehicles," *16th International IEEE Conference on Intelligent Transportation Systems (ITSC 2013)*, pp. 296–301, Oct. 2013. DOI: 10.1109/ITSC.2013.6728248.

[13] A.-L. Schlamp, J. Gerner, K. Bogenberger, and S. Schmidtner, "User-centric green light optimized speed advisory with reinforcement learning," *2023 IEEE 26th International Conference on Intelligent Transportation Systems (ITSC)*, pp. 3463–3470, 2023. DOI: 10.1109/ITSC57777.2023.10422501.

[14] M. Wegener, L. Koch, M. Eisenbarth, and J. Andert, "Automated eco-driving in urban scenarios using deep reinforcement learning," *Transportation Research Part C Emerging Technologies*, vol. Vol. 126, p. 102 967, May 2021. DOI: 10.1016/j.trc.2021.102967.

[15] X. Zhang, X. Jiang, N. Li, Z. Yang, Z. Xiong, and J. Zhang, "Eco-driving for intelligent electric vehicles at signalized intersection: A proximal policy optimization approach," *ISCTT 2021; 6th International Conference on Information Science, Computer Technology and Transportation*, pp. 1–7, 2021.

[16] V. Nguyen, O. T. T. Kim, N. D. Tri, S. I. Moon, and C. S. Hong, "An efficient and reliable green light optimal speed advisory system for autonomous cars," *2016 18th Asia-Pacific Network Operations and Management Symposium (APNOMS)*, pp. 1–4, Oct. 2016. DOI: 10.1109/APNOMS.2016.7737260.

[17] Technische Hochschule Ingolstadt (THI). "Reallabor high definition testfeld (hdt) – projekt kivi." (2026), [Online]. Available: https://www.thi.de/forschung/carissma/labore/reallabor-hdt/ (visited on 02/04/2026).

[18] J. Gerner, D. Rößle, D. Cremers, K. Bogenberger, T. Schön, and S. Schmidtner, "Enhancing realistic floating car observers in microscopic traffic simulation," *2023 IEEE 26th International Conference on Intelligent Transportation Systems (ITSC)*, pp. 2396–2403, 2023. DOI: 10.1109/ITSC57777.2023.10422398.

[19] K. Schleinitz, T. Petzoldt, L. Franke-Bartholdt, J. Krems, and T. Gehlert, "The german naturalistic cycling study – comparing cycling speed of riders of different e-bikes and conventional bicycles," *Safety Science*, vol. 92, pp. 290–297, Feb. 2017. DOI: 10.1016/j.ssci.2015.07.027.

[20] L. Maurer, A. Meister, and K. Axhausen, "Cycling speed profiles from gps data: Insights for conventional and electrified bicycles in switzerland," *Journal of Cycling and Micromobility Research*, vol. 5, p. 100 077, Jul. 2025. DOI: 10.1016/j.jcmr.2025.100077.

[21] P. Huertas-Leyva, M. Dozza, and N. Baldanzini, "Investigating cycling kinematics and braking maneuvers in the real world: E-bikes make cyclists move faster, brake harder, and experience new conflicts," *Transportation Research Part F: Traffic Psychology and Behaviour*, vol. 54, pp. 211–222, Apr. 2018. DOI: 10.1016/j.trf.2018.02.008.

[22] N. Kovácsová, J. C. F. de Winter, A. L. Schwab, M. Christoph, D. A. M. Twisk, and M. P. Hagenzieker, "Riding performance on a conventional bicycle and a pedelec in low speed exercises: Objective and subjective evaluation of middle-aged and older persons," *Transportation Research Part F: Traffic Psychology and Behaviour*, vol. 42, pp. 28–43, Oct. 2016. DOI: 10.1016/j.trf.2016.06.018.

[23] M. Dozza, T. Li, L. Billstein, C. Svernlöv, and A. Rasch, "How do different micro-mobility vehicles affect longitudinal control? results from a field experiment," *Journal of Safety Research*, vol. 84, Oct. 2023. DOI: 10.1016/j.jsr.2022.10.005.

[24] B. 2. (R.) "Sicherheitsabstand: Welchen abstand schreibt die stvo vor?" (), [Online]. Available: https://www.bussgeldkatalog.org/sicherheitsabstand/ (visited on 02/05/2026).

[25] M. Harth, M. Langer, and K. Bogenberger, "Automated calibration of traffic demand and traffic lights in SUMO using real-world observations," in *SUMO Conference Proceedings*, 2022, pp. 133–148. DOI: 10.5282/ubm/epub.93405.

[26] M. Behrisch, L. Bieker, J. Erdmann, and D. Krajzewicz, "Sumo - simulation of urban mobility: An overview," *The Third International Conference on Advances in System Simulation*, 2011.

[27] Nachhaltigkeitsagenda Ingolstadt. "11 - nachhaltige städte und gemeinden: Indikator 11.17: Modal split." (2026), [Online]. Available: https://sdg.nachhaltigkeitsagenda-ingolstadt.de/11-17/.

[28] A. Roosta, H. Kaths, M. Barthauer, J. Erdmann, Y.-P. Flötteröd, and M. Behrisch, "The state of bicycle modeling in sumo," in *SUMO Conference Proceedings*, vol. 4, Hannover, Germany: TIB Open Publishing, 2023, pp. 55–64. DOI: 10.52825/scp.v4i.215.

[29] S. Krauß, P. Wagner, and C. Gawron, "Metastable states in a microscopic model of traffic flow," *Physical Review E*, vol. Vol. 55, no. 5, pp. 5597–5602, May 1997. DOI: 10.1103/PHYSREVE.55.5597.

[30] Zweirad-Industrie-Verband e.V. "Ziv market data presentation 2025 for 2024." (2025), [Online]. Available: https://www.ziv-zweirad.de/wp-content/uploads/2025/03/ZIV-Market-Data-Presentation-2025-for-2024.pdf.

[31] C. M. Konrad, A. Dabiri, F. Schulte, J. K. Moore, and R. Happee, "Cycling safety assessment in microscopic traffic simulation: A review and methodological framework," *Transportation Research Interdisciplinary Perspectives*, vol. 34, p. 101 734, 2025. DOI: 10.1016/j.trip.2025.101734.